Contribution of Phonon Anharmonicity in Negative Thermal Expansion Materials

Aashna Jain, and Pallavi Ghalsasi*

School of Engineering and Technology, Navrachana University, Vasna-Bhayli Road, Vadodara- 391410, Gujarat, India

Received: 28 July 2021 Revised: 25 December 2021 Accepted: 25 January 2022 Published: 25 March 2022

*Corresponding Author: pallavig@nuv.ac.in

Abstract:

A crystal lattice of a solid consists of periodic arrangement of atoms. The atoms in the lattice vibrate about their allotted positions at normal temperatures. These atomic vibrations generate sound waves in the crystal lattice. According to the quantum theory, analogous to Photons-light particles, the particle *avatar* of these sound waves are called as Phonons. In reality, the vibrations of atoms in a crystal lattice deviate from their harmonic rhythm as a function of temperature. This anharmonic behavior affects the atoms ability to help flow heat seamlessly throughout the solid with varying temperature. This in turn is responsible to the fact whether and how much the solid should expand with increase in temperature. Present paper intends to understand the crystalline solids which shrink when heated instead of usual expansion. The cause of this so called 'Negative Thermal Expansion' can be explained by anharmonic behavior of the phonons. We present a few of the various approaches adopted in literature to study the contribution of anharmonicity in thermal expansion.

Keywords

Anharmonicity, Negative Thermal expansion, Grüneisen parameter, Phonon, Specific heat, Lattice dynamics

Introduction

The vibrations of atoms in a solid are interpreted as elastic waves or acoustic waves propagating through the solid. These vibrations rely on crystal symmetry, number of atoms per unit cell, chemical bonding and presence of crystal defects in a solid. The displacement of atoms in this oscillatory behavior will be greater at high temperatures. Forces holding these atoms in their equilibrium positions are proportional to their relative displacements mimicking their network with neighboring atoms by springs.

Phonons and Specific Heat:

When the temperature is raised above absolute zero there is a rapid increase in the specific heat from zero which eventually becomes constant (C=3NK; K= Boltzmann constant). Dulong and Petit stated that this value at high temperature is about 6 cal $mole^{-1}$ $degree^{-1}$. According to Dulong and Petit law, a solid has 3R molar heat capacity at constant volume developed with the help of the equipartition theorem of Boltzmann. This model failed to explain the drop of specific heat value for solids at low temperatures and was overcome by involving quantum aspect introduced by Einstein[1].Einstein assumed that all the atoms in a solid vibrate at same frequency. The frequency of the atom can be effected by restoring force and mass of the atom. Einstein model replaced the classical law of equipartition with the mean energy of Planck's oscillator. The specific heat at constant volume for Einstein model where all the atoms of a crystal were assumed to be N harmonic oscillators having same frequency (ν) is given by,

$$C_v = 3NK_B \left(\frac{h\nu}{K_B T}\right)^2 \frac{exp\left({}^{h\nu}/_{K_B T}\right)}{\left[exp\left({}^{h\nu}/_{K_B T}\right) - 1\right]^2} \qquad (1)$$

At high temperatures, $T \gg {}^{h\nu}/_{K_B}$, above expression reduces to the Dulong-Petit value of the specific heat . On the other hand, at low temperatures i.e.$T \ll {}^{h\nu}/_{K_B}$, $C_v$tends to zero for T approaching to zero Kelvin and it increases with increasing temperature as required by third law of thermodynamics. This model was improved by Debye by assuming solid to be a continuous medium rather to be a discrete one and accounting for the range of frequencies in a solid instead of assuming same frequency of oscillation for all the atoms, as claimed by Einstein[2,3]. Debye Specific heat is given by

$$C_v = 3NK_B\left(\frac{3}{x_D^3}\int_0^{x_D}\frac{x^4e^4dx}{(e^x-1)^2}\right); x_D = {h\nu_D}/{K_BT} \qquad (2)$$

$$= \frac{T_D}{T}\ ; T_D\ is\ Debye\ temperature$$

The above expression reduces to Dulong-Petit law at high temperatures whereas for low temperatures, Debye specific heat decreases as T^3. Figure1 shows the typical variation of $C_v$as a function of temperature for Debye model and Einstein models where all the harmonic oscillators vibrate at the same frequency.

To examine the Debye model, one can have a resemblance with a particle in a cubic box. Equation (2) suggests that T_D decides the complexity in the integration of above expression. The smallest dimension in a solid (i.e. a unit cell) decides the minimum wavelength of the atoms performing lattice vibration and thereby setting up a limit for maximum thermal vibrational energy for the atoms in a solid which in turn model into an independent normal mode vibration[4]. The internal energy possessed by the atoms in such a condition is expressed as

$$U_{thermal} = 3nN_AK_BT = 3nRT \qquad (3)$$

Where n, N_A, K_B, T, and$R$ are the mole number, Avagadro number, absolute temperature and Universal gas constant respectively. The T_D defined in equation (2) describes the temperature at which ordered lattice vibration turns into an independent lattice vibration.

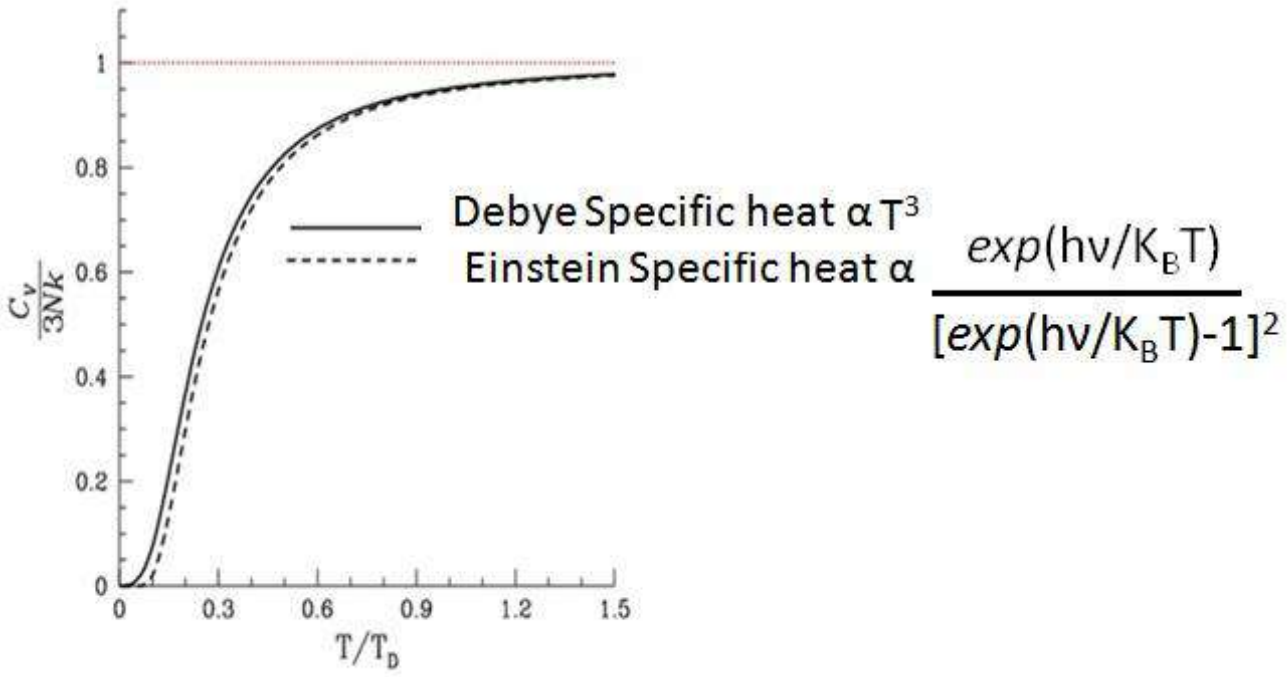

Figure 1: Comparison of Debye and Einstein Specific Heat Curve[5]

Retrieved from https://commons.wikimedia.org/wiki/File:DebyeVSEinstein-ruRu.png
This file is made available under the Creative Commons CC0 1.0 Universal Public Domain Dedication

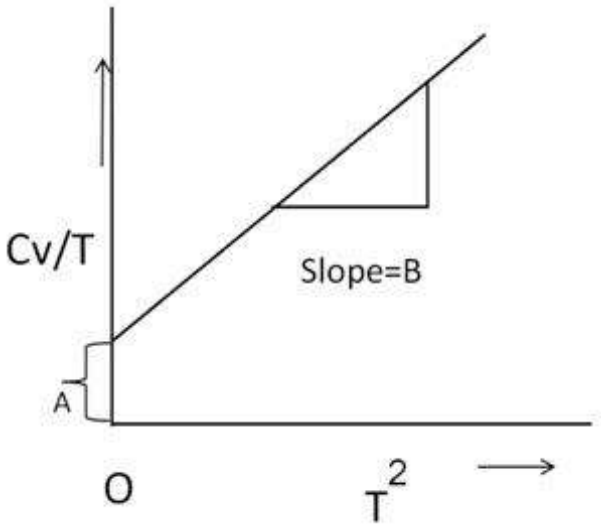

Figure 2: Debye Specific heat curve for metals[2]

In case of metals, the total contribution of specific heat involves specific heat of free electrons in addition to that of phonons and it is given by,

$$C_{V=}\ AT(C_{V_{(free\ electrons)}}) + BT^3(C_{V_{(phonons)}}) \qquad (4)$$

C_v/T verses T^2 graph (Figure2) shows that the linear plot which allows to determine Debye frequency by calculating the slope value (B) and intercept (A) determines the contribution to the specific heat by the electrons across Fermi level in a metal which is known as electronic specific heat coefficient[2].

Phonons and Heat Conduction:

In this section, we describe the heat conduction due to phonons in insulators. Thermal conduction in insulators occurs as a result of exchange of energy and momentum termed as phonon-phonon collisions. The thermal conductivity of a material is dependent on the specific heat per unit volume (C_V), phonon velocity(v) and phonon mean free path(l).When the atoms of a solid material experience purely harmonic forces then the phonon-phonon collision do not occur. This means that there will not be any scattering between the phonons even for a finite temperature. As a result, there is no occurrence of thermal resistance (i.e. infinite thermal conductivity) in the case of solids with harmonic approximation. By contrast, phonons get scattered with one another when the atoms in a solid experience anharmonic forces. The distribution of phonons gets disturbed for an anharmonic solid when there is a temperature gradient. Consequently, phonon-phonon interactions or scattering take place in the system in order to acquire their equilibrium distribution back. The rate at which the equilibrium distribution is regained decides the thermal resistance of the material. This rate of attaining equilibrium distribution is dependent on the phonon-phonon scattering. At low temperatures, only low energy phonons get excited. Such phonons corresponding to longer wavelengths experience scattering across the boundary of the material. In this case, C_V varies as T^3 as discussed in the above section and l is nearly constant. Moreover, the velocity of phonon is not sensitive with varying temperature. Consequently, the thermal conductivity varies as T^3 at low temperatures but once the temperature is reached to $\frac{T_D}{2}$, the thermal conductivity varies as $1/T$ since at high temperatures, C_V is nearly constant and l decreases with the magnitude of $1/T$.At high temperatures, phonon-phonon collisions dominate due to the anharmonicity established

in the solid material. Hence, "anharmonicity" of the lattice vibrations plays the vital role to the thermal resistance of a system[2]. In case of metals, free electrons are available in abundance which efficiently conducts heat transfer resulting into high thermal conductivity into metals.

Umklapp process helps to understand the mechanism of thermal resistivity conducted by phonons. The Umkalpp process commonly known as flipping over says that in the phonon-phonon collision the total momentum of the system is changed after the collision. When two different phonons with momentum $\hbar q_1$ and $\hbar q_2$ collide, the total momentum of the system is given as $\hbar q_3$with a difference of the material's lattice parameter vector (G). This phenomenon can mathematically express as follows:

$$k_1 + k_{1=}\ k_3 + G \qquad (5)$$

In case of normal scattering (N-process), total momentum is conserved. The vector G= 0 in this situation and there is no prominent variation in the direction of energy. Hence, such a normal process cannot contribute towards thermal resistance. By contrast, in Umklapp process (U-process), one can notice peculiar variation in the energy direction (in the direction of k-vector) resulting in thermal resistance of the system (Figure3). As shown, resultant phonon vector(k_3 vector)for N-process lies within 1st Brillouin zone of 1D k-space and this moves outside of 1stBrillouin zone (k_3') for U-process. The G vector describes the distance between two lattice phonons and G= 2π/a for 1D k-space[2].

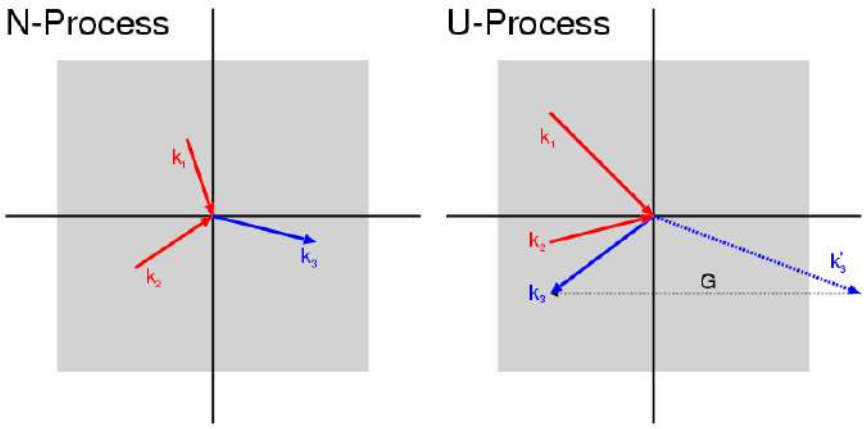

Figure 3: Umklapp process in a solid[6]

Retrieved from https://commons.wikimedia.org/wiki/File:Phonon_nu_process.png

This image was marked with licensed under CC BY-SA 3.0

Lattice Vibrations:

For a 1D lattice infinitely extended in the X-direction of identical atoms having mass m and interatomic separation a, the equation of motion of the n[th] atom can be represented as:

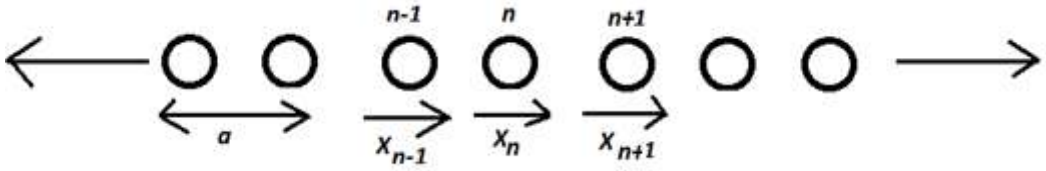

Figure 4: Monoatomic lattice vibrations in a 1D infinite solid[2]

$$m\frac{d^2x_n}{dt^2} = -f(x_n - x_{n+1}) - f(x_n - x_{n-1}) \quad (6)$$

Where, x_n, $x_{n+1}$and $x_{n-1}$are the displacements of the n^{th} atom and its nearest neighbor atoms at $(n\text{-}1)^{th}$ and $(n+1)^{th}$ positions. 'f' is the force constant of the interacting $(n\text{-}1)^{th}$ and $(n+1)^{th}$ atoms. The solution to the above equation takes the form of running wave as follows:

$$x_n(t) = Ae^{-j(\omega t - qna)} \quad (7)$$

$$x_{n+1}(t) = Ae^{-j[\omega t - q(n+1)a]} \quad (8)$$

$$x_{n-1}(t) = Ae^{-j[\omega t - q(n-1)a]} \quad (9)$$

Where ω and q describe the frequency and the wave vector of the elastic wave. Putting the above obtained solutions into the equation of motion, one can determine the frequency of the elastic waves called as dispersion relation given by,

$$\omega = \sqrt{\frac{4f}{m}}\sin\left(\frac{qa}{2}\right) \quad (10)$$

The atoms of an elastic wave are considered in accordance to the quantum laws. The quantized excitations in such an elastic wave due to the virtue of thermal vibrations are called Phonons.

The energy of the atoms of the elastic wave is taken as discrete since atoms are quantum particles and its smallest unit is termed as "Phonon". The medium can be approximated as a

continuum in the limit of long wavelength phonons ($\lambda >> a$) reducing the dispersion relation to $\omega = \sqrt{\frac{4f}{m}}\ (\frac{qa}{2})$(since qa<<1). The relation between frequency (ω) verses wave vector (q) (Equation 10) states that ω has a periodicity of $q=2\pi/a$. The unique values of ω are limited to a range of q within 2π/a. The range of q lying between $-\pi/a$ to $+\pi/a$ is called the first Brillouin zone[2].

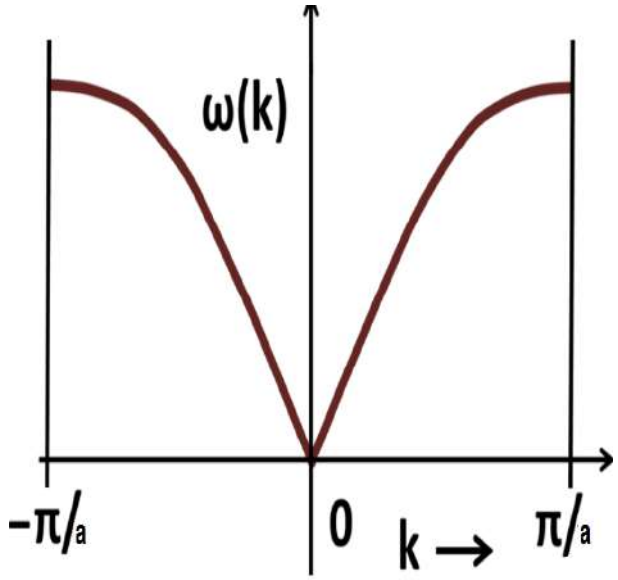

Figure 5: Dispersion Curve of a Monoatomic Lattice[7]

Retrieved from https://search.creativecommons.org/photos/7cfa6c60-b1a4-415c-bf5f-8bfaf43de579. This image was marked with a CC BY-SA 3.0 license.

In general, for an infinite lattice chain of two different types of atoms is considered then the dispersion relations are classified into ranges and can be expressed as follows:

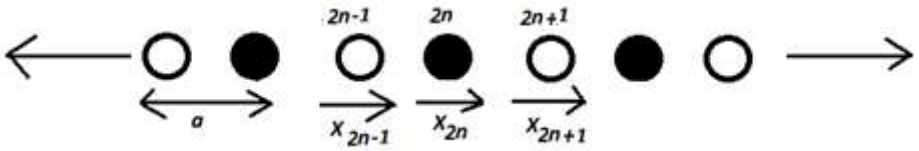

Figure 6: Diatomic lattice vibrations in a 1D infinite solid[2]

$$\omega_+ = \left[f\left(\frac{1}{M}+\frac{1}{m}\right) + f[(\frac{1}{M}+\frac{1}{m})^2 - \frac{4sin^2qa}{Mm}]^{1/2} \right]^{1/2} \quad (11)$$

$$\omega_- = \left[f\left(\frac{1}{M}+\frac{1}{m}\right) - f[(\frac{1}{M}+\frac{1}{m})^2 - \frac{4sin^2qa}{Mm}]^{1/2} \right]^{1/2} \quad (12)$$

Where M and m are the masses of two different types of atoms with force constant f and wave vector q. The dispersion curves for ω_+ and ω_-(as shown in Figure7)states that ω_+ includes high frequency range of phonon modes categorized as Optical phonons while ω_- includes low frequency range of phonon modes termed as Acoustic phonons[2].

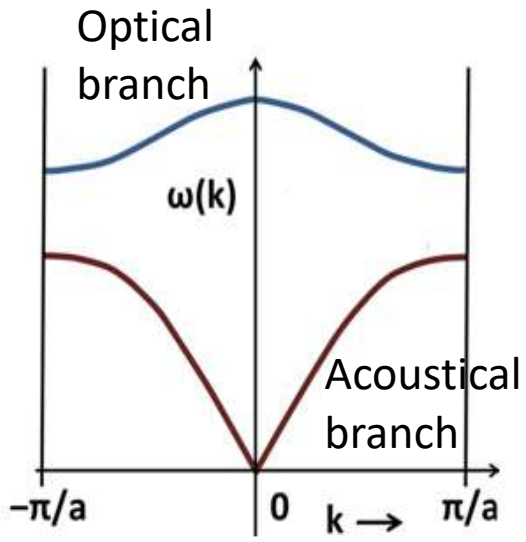

Figure 7: Dispersion Curve of a Diatomic Lattice[8]

Retrieved from https://search.creativecommons.org/photos/e241e9a9-aa09-490f-a4ab-cdbe6829cf3e

The oscillation of atoms about their equilibrium positions becomes more intensive at high temperatures. This can influence several properties in a solid such as specific heat, thermal conductivity and thermal expansion as discussed below.

Phonons and Thermal Expansion:

A solid undergoes a thermal expansion upon heating which is a direct consequence of anharmonicity of lattice vibrations. For a solid having perfectly harmonic vibrations, the mean position of the oscillator does not get shifted with increasing temperature. But the atomic oscillators in general, have an asymmetric anharmonic potential. In such cases, atoms possess higher energy and consequently greater amplitude of vibration at higher temperatures. The mean position of the atom then shifts towards the right at higher temperatures in order to obtain the symmetric amplitude of vibration. Due to this shifting of the equilibrium position of each atom in the lattice, the mean interatomic separation increases as shown in the Figure No.8. This causes increase in the dimension of the material with a positive coefficient of thermal expansion $(\alpha)^2$.

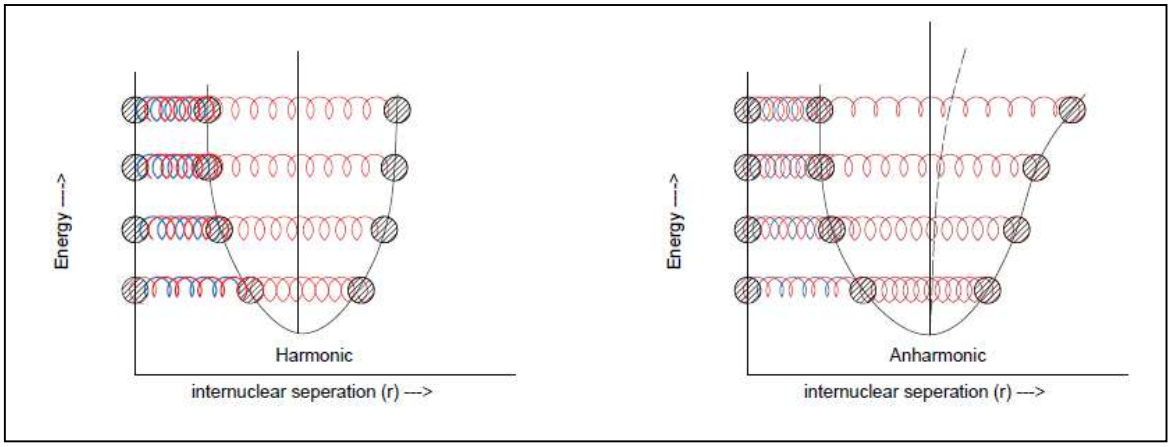

Figure 8: Spring Model for Vibrations of a Solid (Blue: compressed spring, Red: Stretched spring

Researchers have been studying the phonons behavior as a function of temperature over the decades. It is observed that not every material undergoes expansion upon heating but some materials contract when heated. Such materials have been named as Negative Thermal Expansion(NTE) materials. Anharmonicity in phonon mode frequencies plays a vital role for such an unusual thermal behavior in this class of materials. The phonon mode frequency variation with respect to temperature at constant pressure is a combined contribution of two effects: 1. True anharmonicity (also called as explicit anharmonicity) which occurs due to the change in vibration amplitudes at fixed equilibrium positions. 2. Quasi-anharmonicity (also

called as implicit anharmonicity) resulting from volume change with respect to pressure at constant temperature. The total anharmonicity in a solid can be represented mathematically as

$$\frac{1}{\omega_j}\frac{d\omega_j}{dT}\Big|_P = \frac{1}{\omega_j}\frac{d\omega_j}{dT}\Big|_V - \gamma_j\alpha \qquad (13)$$

γ and α (measured in K^{-1}) in the quasi-term is the Grüneisen parameter and coefficient of thermal expansion respectively and can be computed as follows

$$\gamma_j = -\partial \ln \omega_j / \partial \ln V \qquad (14)$$

$$\alpha = V^{-1}(\partial V/\partial T) \qquad (15)$$

The first term in Equation 13, on right hand side is the true anharmonicity and second term is the quasi-anharmonicity. The contribution of these two terms is responsible for the total anharmonicity of the phonon modes expressed on left hand side in the above equation. For a typical positive thermal expansion material (PTE), vibration frequency red shifts with increase in temperature making the left side of the above equation negative. Normally, the first term on the right hand side is also negative and with positive values of γ and α, even the second term on the right side of the equation is negative.

For NTE materials, change in the sign of γ_i in the equation13 may result in the overall sign change of total anharmonicity[9, 10].The average Grüneisen parameter (γ_{AV}) at constant volume is related to α as follows

$$\alpha = \frac{\gamma_{AV} C_V}{3V_m B} \qquad (16)$$

Where V_m is the molar volume, $B$is the Bulk Modulus and $C_V$is the specific molar heat at constant volume given by,

$$C_V = \frac{1}{N}\sum p_i C_i \qquad (17)$$

Where N is the number of formula units per unit cell,p_i is the number of phonons having frequency $\omega_i$andC_i is the single mode specific heat.

One can calculate average Grüneisen parameter (γ_{AV}) by the following expression

$$\gamma_{AV} = \left(\frac{1}{N}\sum p_i C_i \gamma_i\right)/C_V \qquad (18)$$

It can be noticed from above equations that for the material with negativeγ_{AV}, α has to be negative confirming it as NTE material[10].

Major Advancements:

Present article attempts to present various methods often found in literature that can be helpful in understanding the phonon behavior in NTE materials.

1. ***Experimental Methods:***

   Experimentally temperature dependent inelastic neutron scattering experiments and temperature and/or pressure dependent Raman measurements on NTE materials have proven to be very fundamental to assess role of phonons in negative thermal expansion property in these materials.

   In-elastic Neutron scattering technique involves exchange of both energy and momentum of thermal neutrons with moving nuclei, hence giving information about atomic vibrations. This scattered cross-section corresponding to the characteristic of the system provides the information about the phonons of the sample. It gives an idea whether the scattering is due to a one phonon process or multi-phonon process. Moreover, for the case of incoherent approximation this method can give neutral weighted density of states of the powdered sample scattering once the weighting of the total scattering crossection of the constituent atoms is determined[11].From the Inelastic neutron scattering data, one can extract phonon dispersion relation and phonon density of states. This can further be used to determine quantitative thermodynamical response and phase information inmaterials[12].

   The phonon behavior of the very popular NTE material, zirconium tungstate (ZrW_2O_8) has been extensively studied based on this method and below we overview these studiesZrW_2O_8shows isotropic NTE over a wide temperature range from 0.3K to 1050K. The structure contains 3-dimensional network of ZrO_6 and WO_4polyhedra with one non-bridging Oxygen atom present on each WO_4 tetrahedron which undergoes a transverse vibration exhibiting rigid unit mode[13].

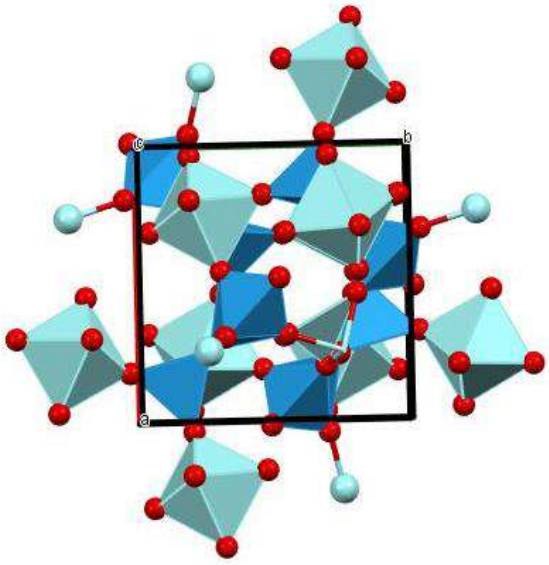

Figure 9: The crystal structure of ZrW_2O_8[13]: (color online). Red: oxygen, Blue: tungsten, Green: zirconium

Inelastic neutron scattering measurements:

Neutron scattering studies by Ernst et al.[14]had traced two groups of phonons: low energy phonons (at 30meV) and high energy phonons (at 110meV). Since there are 4 formula units of ZrW_2O_8 per unit cell, there are total 44 x 3 = 132 vibrational modes, out of which 3are the acoustic modes and 129 are the optical modes. These modes were determined and subjected to investigation of their contribution to NTE. γ_i for low energy phonons were obtained from equation (16) and (17) with negative magnitude as a function of temperature. Moreover, large negative γ_i indicating the frequency red shift as a function of pressure were analyzed for low phonon energies. Inelastic neutron scattering data showed linear decrease in lattice parameter 'a' with increase in temperature, whereas inverse dependence of Grüneisen parameter γ with temperature except some deviation at low temperatures[14]. Considering these aspects, a model was proposed as shown in the inset of Figure10, wherein the low energy phonons lying between E_0(1.5meV) and E_1(8.5meV) were assumed to be responsible for the temperature dependence of theγvalues. Phonons having energies between E_0 and E_1, were assumed to have fixed γ= -14. This model was supported satisfactorily with the help of the density of states g(ω) values. Further g(ω) verses $\hbar\omega$ plot was analyzed for

these set of phonon modes at 50K and 300K. This Low energy spectrum shows hardening for 3.8meV mode with increasing temperature contradicting the assumption that frequency depends only on volume and not on temperature. It is known that the difference in energy increases for every adjacent eigen states with the increasing eigen state index in the case of quartic anharmonic harmonic oscillator. This in turn results into increment of the average eigen states spacing[14].In ZrW_2O_8, the structural orientation of unshared vertex of tetrahedron and large experimental values of $C_V$can lead to the similar variation in the energy of the lattice. Hence it was interpreted that hardening of 3.8meV is the result of dominancy of the quartic potential of the oscillator[14].

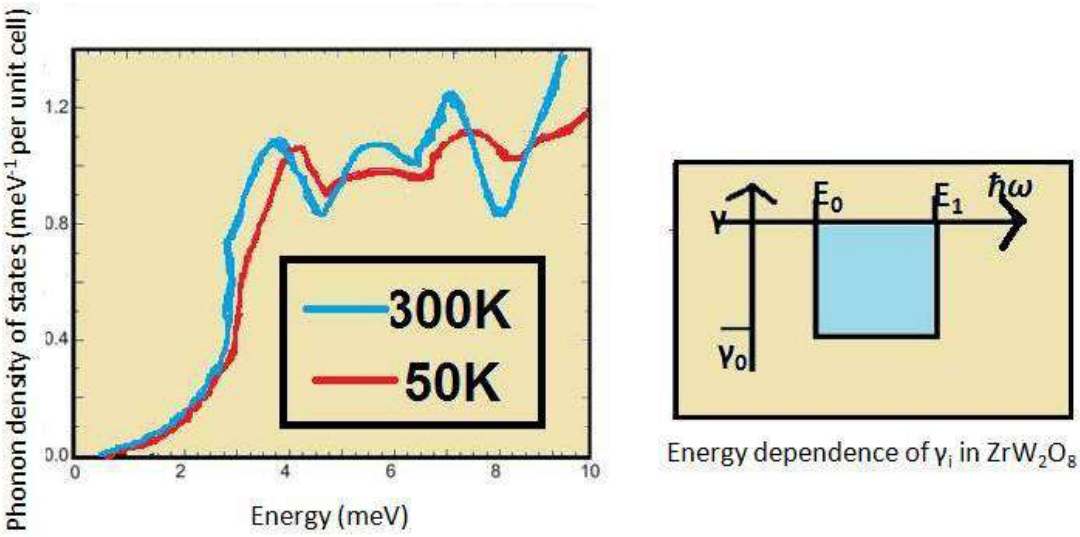

Figure 10: Variation of density of states with low-energy at temperatures 50K, and 300K[14].

Re-drawn from "Ernst, G., Broholm, C., Kowach, G. R., & Ramirez, A. P. (1998). Phonon density of states and negative thermal expansion in ZrW 2 O 8. *Nature*, *396*(6707), 147–149."

Specific heat measurements:

Phonon spectrum and specific heat at low temperature depends upon the atomic masses and bonding forces especially on bonding with neighboring atoms, coordination

number and symmetry of adjacent atoms. The change in the coordination number can result into the structural change of a system. Hence, $C_v(T)/T^3$ vs lnT plot can satisfactorily explain the contributions of $C_v(T)$ for the various different modes in a system[15]. This plot also overlaps approximately with the one dimensional phonon density of states with energy (Ref15) For ZrW_2O_8, $C(T)/T^3$ vs lnT plot was interpreted for spectral weight of low energy phonons using fitting protocols of Einstein and Debye and it was stated that these phonons can be associated to structural transition and liberation of atoms. The former protocol assumes the individual contribution of summation of Einstein phonons while the latter protocol assumes higher Debye temperatures to fit for C_V.After trials of various combinations, it was found that the protocols lead to the ~6.5% fraction of the total degrees of freedom spectral weight for the phonon modes residing at 5meV in ZrW_2O_8 giving out the signatures of order-disorder transition[15].This kind of transition was further understood with an analogy of 'guitar string' as given below.

In ZrW_2O_8, the underconstrained or unshared vertex (non-shared O atom in WO_4) leads to the order-disorder transition. By contrast, ZrO_6 has completely shared oxygen performing a transverse vibrational motion. In addition, the negative sign of γ_i of low energy phonons were also indicating this transverse behavior in analogy to the 'guitar string' wherein a heavy mass suspended between the strings tends to pull in the string support resulting in the shrinkage of the overall structure. So, the transverse vibration of rigid unit modes (RUMs) of low energy phonons plays the key role in ZrW_2O_8 for showing up the unusual NTE property. Low energy phonons show large softening in case of HfW_2O_8 and $ZrMo_2O_8$ consisting of isotropic NTE up to 1050K and 600K respectively. Evidences proved that the guitar string analogy holds true in these two compounds like ZrW_2O_8[15, 16, 17, 18].

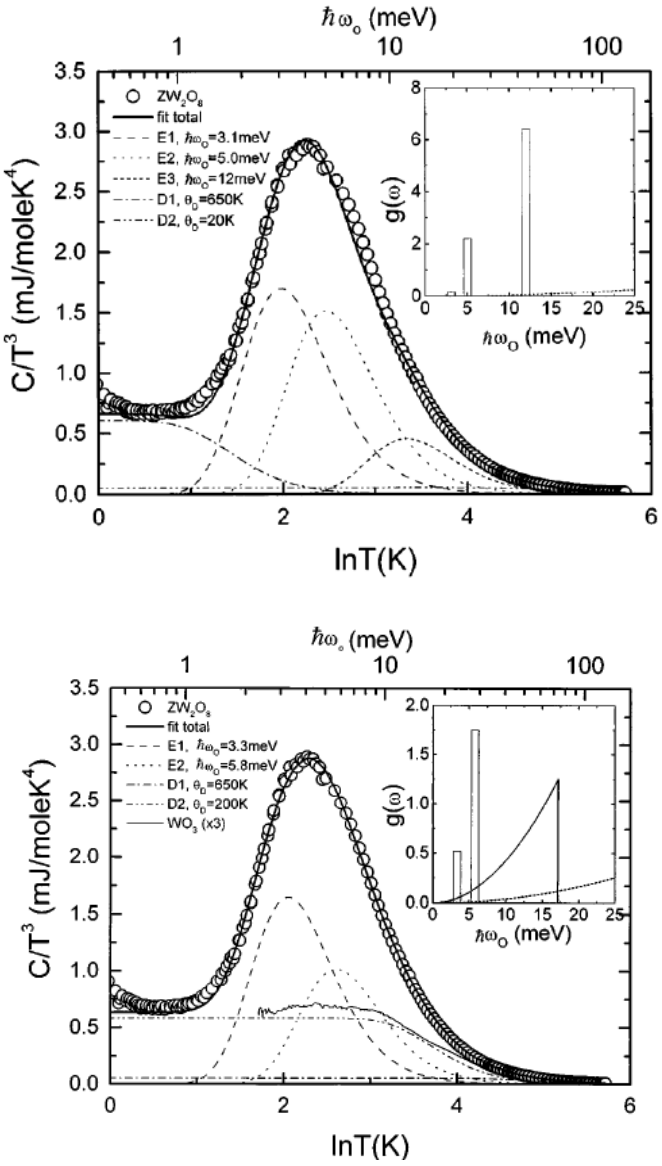

Figure 11: $C_v(T)/T^3$ vs lnT plot of ZrW_2O_8 as per the Einstein and Debye protocols[15].

"Reused (figure 3 and 4) with permission from [Ramirez, A. P., & Kowach, G. R. (1998). *Atomwork http://crystdb.nims.go.jp/*. 4903–4906.] Copyright (1998) by the American Physical Society."

Thermal properties of Metal cyanides are of keen interest to the scientists. $Zn(CN)_2$ consists of a pairing of strong C≡N bonds to weak Zn-C/N bonds enabling transverse vibration of Zn-CN-Zn linkages which is the key factor for NTE behavior in this material. It has cubic structure available in two different models namely ordered model

with space group $P\bar{4}3m$ and disordered model with $Pn\bar{3}m$ space group. The former one is having ZnC_4 and ZnN_4tetrahedra around the alternate cations along with CN ions arranged in an orderly fashion residing along the body diagonal of the unit cell. By contrast, the distribution of C and N atoms is oriented randomly in order to meet the site probabilities to be in equal amount. By contrast, disordered model offers equal sites occupancy with the help of randomly distributed C and N atoms[19].

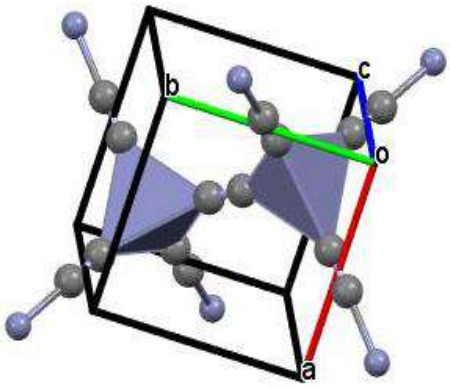

Figure 12: The crystal structure of $Zn(CN)_2$ [20]

High pressure neutron scattering technique reported that the low energy (less than 15meV) phonons cause NTE in $Zn(CN)_2$ by plotting the energy variation of these modes with ratio of calculated γ_i/B; B is Bulk modulus, at an ambient pressure for 165K and 225K temperatures. The γ_i/B ratio obtained from ab-initio calculations were analyzed to observe the anharmonicity of phonons. Using the high pressure neutron scattering data γ_i/B ratio and energy of the low phonon modes, α was determined and it was confirmed that this set low energy of phonons corresponds to NTE. Moreover, temperature and pressure dependency of $Zn(CN)_2$ over atomic displacement parameters indicated the softening of the modes along Zn-CN-Zn transverse linkages which is the key compression mechanism for this material[21,22].

Raman Spectroscopy is a powerful technique when performed on the sample under temperature or pressure constraints as it allows to probe into true and quasi-anharmonic contributions of phonons (in equation13 of total anharmonicity). Further, the contribution of anharmonicity of three phonon process and four phonon process can be determined with true anharmonicity calculations as per Equation No-19 which describes the variation/shift in the frequency of the phonon due to its phonon-phonon anharmonic

contribution $\left(\Delta\omega_j(T)_{anh}\right)$.This equation shows that each phonon frequency (ω) can be characterized into two (ω_m, =1, 2) or three (ω_n, =1,2,3) phonons resulting into three (cubic) and four(quartic) phonon processes. Coefficients A and B describe the strength of three and four phonon processes respectively[23,24]. The frequency variation of phonon modes in a material against temperature and pressure determines the magnitude of α and γ respectively. One can obtain information of α with the help of phonon frequency variation with respect to temperature (refer equation no 15). On the other hand, phonon frequency variation as a function of pressure helps to obtain γ information (refer equation no 14). The calculation of Bulk modulus requires knowledge of γ, which can be deduced from high pressure Raman studies. The study of phonon anharmonicity of certain materials namelyZrW_2O_8, $Ag_3Co(CN)_6$, SnSe, 2H-WS_2 have been discussed below. It has been noticed that major contribution in total anharmonicity is brought by true anharmonicity in the above listed materials.

$$\Delta\omega_j(T)_{anh} = A[1 + \sum_{m=1}^{2} \frac{1}{e^{\hbar\omega_m/K_BT} - 1}] + B[\,1 + \sum_{n=1}^{3} \left(\frac{1}{e^{\hbar\omega_n/K_BT} - 1} + \frac{1}{\left(e^{\hbar\omega_n/K_BT} - 1\right)^2} \right)] \qquad (19)$$

Zirconium tungstate has been reported to have an order-disorder phase transition from $P2_13$(α-phase) to $Pa\bar{3}$ (β- phase) with respect to temperature (at 428K). This phase transition can be the result of anharmonicity in the phonon modes. High pressure Raman spectroscopic study of zirconium tungstate (crystal structure discussed above) was performed from 20K -400K for α-phase. Low frequency modes related to tungsten ion and WO_4tetrahedra and high frequency modes related to only WO_4tetrahedra were traced. In order to examine their behavior closely, phonon frequencies' variation with respect to temperature was analyzed. The slope of each mode reflects the anharmonicity in these modes. The disappearance of certain modes below 400K confirmed the phase transition in the material. Previous reports indicated negative Grüneisen parameters (γ_i) for phonons with energies less than 50meV.Temperature dependent specific heat shows that phonons

much larger than 10meV contributes for NTE apart from low energy phonons (less than 10meV) reported earlier[14,15,16]. Analysis of phonon frequencies variation as a function of temperature and the linewidths were studied to distinguish between true and quasi-anharmonicity. In the literature, $\Delta\omega_j(T)_{anh}$ and FWHM (Γ) are related[25] as follows:

$$\lim_{\delta\to 0} -\frac{1}{K_B T}\sum(kj;\omega \pm i\delta) = \Delta\omega_j(T)_{anh} \mp i\Gamma_j \qquad (20)$$

Where δ, k and j describe the phonon phase, wave vector and j^{th} indexphonon branchrespectively.

Previous reports have given the formalism for cubic and quartic anharmonicities describing three- and four- phonon processes with respect to the FWHM (Γ) as a function of temperature. The cubic and quartic linewidths contributions can be deduced from the equations (21) and (22). A and B define the coefficients of cubic and quartic anharmonicities respectively[23, 24]. For Zirconium tungstate, the quantity called intrinsic linewidth (A+B), bending modes showed large magnitude indicating strong anharmonicity. This corroborated the temperature dependence specific heat results giving out negative γ_i for low frequency modes. Calculated values for true and quasi-anharmonicity using these γ_i confirms true anharmonicity has a larger magnitude corresponding to many lattice modes and some bending modes of tungsten ion in comparison to stretching modes of tungsten ion. Thus, the true anharmonicity of the phonons dominates in the NTE behavior of this material[10]

$$\Gamma_C = A\left\{\left[\exp\left(\frac{\hbar\omega_0}{2k_B T}\right)-1\right]^{-1} + \frac{1}{2}\right\} \qquad (21)$$

$$\Gamma_Q = B\left(\left\{\left[\exp\left(\frac{\hbar\omega_0}{3k_B T}\right)-1\right]^{-1} + \frac{1}{2}\right\}^2 + \frac{1}{12}\right) \qquad (22)$$

Mode Frequency(cm^{-1})	**Total Anharmonic (10^{-5} K^{-1})**	**Quasi-anharmonic $\alpha\gamma_j$ (10^{-5} K^{-1})**	**True Anharmonic (10^{-5} K^{-1})**
41	12(5)	15(3)	27(8)
64	-35(1)	-3(2)	-38(3)
84	-29(6)	7.4(2)	-22(6)
144	2.5(9)	3.5(2)	6(1)
236	3(1)	-2(1)	1(2)
308	2.9(7)	1.7(9)	5(2)
333	2.1(3)	0.4(5)	2.4(8)
381	0.6(2)	0.7(8)	1(1)
735	-0.3(1)	-0.2(6)	-0.5(7)
746	-0.8(3)	-1(1)	-2(1)
773	-2.3(2)	-0.1(3)	-2.4(5)
789	-2.5(1)	-1.0(3)	-3.5(4)
861	-1.0(2)	-0.8(7)	-1.8(4)
886	-1.2(2)	0.0(3)	-0.6(2)
903	-1.68(7)	-0.1(3)	-3.2(6)
932	-0.62(4)	-1.4(4)	-0.6(2)
967	-1.8(2)	-0.8(2)	-3.2(6)
1018	-1.1(3)	-0.8(2)	-1.9(5)
1030	-1.3(1)	-0.8(2)	-2.0(3)

Table 1: Anharmonicity offered by various phonon modes of ZrW_2O_8[10].

"Reused (figure 3) with permission from [Ravindran, T. R., Arora, A. K., & Mary, T. A. (2003). Anharmonicity and negative thermalexpansion in zirconium tungstate. *Physical Review B - Condensed Matter and Materials Physics*, *67*(6), 1–4.] Copyright (2003) by the American Physical Society."

Table1 describes the total anharmonicities of the phonon modes of zirconium tungstate offered by their quasi-anharmonic and true anharmonic components as explained in equation11[10]. One can observe that the most of the low frequency modes shows positive

total anharmonicities. It was known that out of 41, 64, 84, 144 and 308cm^{-1}, only 64 cm^{-1}mode was the only one with positive γ but all of these low phonon modes were having large magnitudes of total anharmonicity. Considering the case of 64cm^{-1} mode, having γ to be positive turns the quasi-anharmonic contribution to be negative value as the corresponding thermal coefficient for this material is negative only for all the modes. Further, the calculated true anharmonicity contribution was found to be negative which when combined with the calculated quasi-anharmonic component turns total anharmonicity to be negative. In a similar manner, one can understand the effect of anharmonicity offered by rest of the phonon modes.

Raman Spectroscopy and X-ray Diffraction Measurements:

$Ag_3Co(CN)_6$ exhibits 14 times larger NTE than ZrW_2O_8. This colossal NTE material consists of alternating layers of Ag atoms sitting over a Kagome lattice and $Co(CN)_6$ lies above and below of it forming Co-CN-Ag-NC-Co linkages[26].

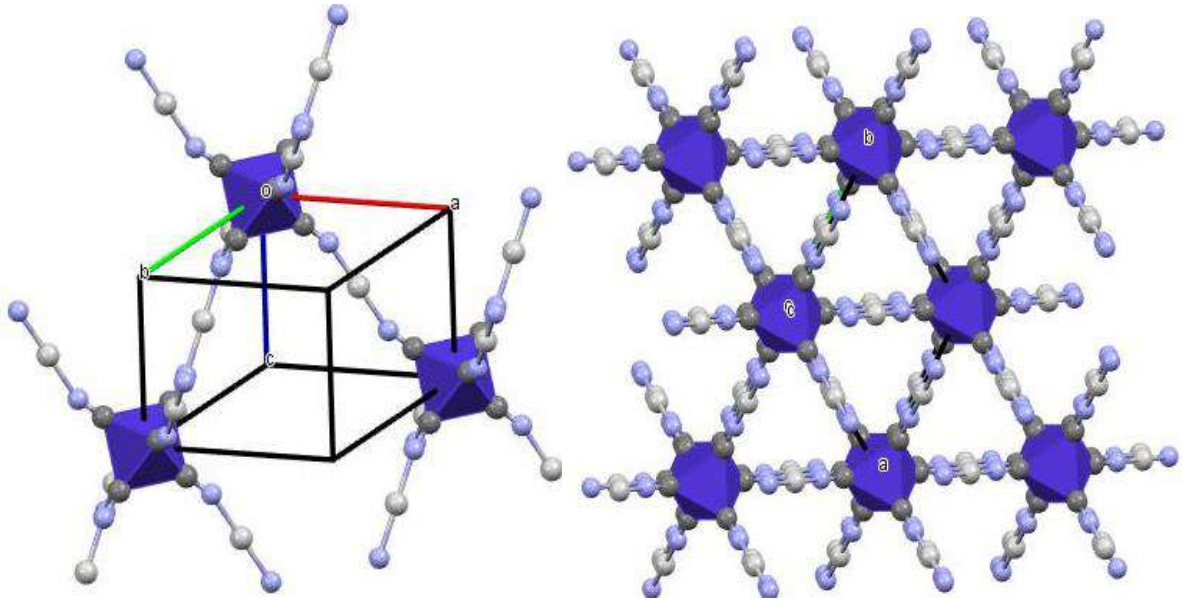

Figure 13: The crystal structure of $Ag_3Co(CN)_6$[27]

High pressure Raman studies of $Ag_3Co(CN)_6$ studies was performed to understand the anharmonic behavior of phonons in this material. Soft phonons were traced by pressure dependence of phonon modes and they possessed negative γ_i. Moreover, quasi-anharmonic contribution of these modes was obtained from frequency variation as a function of

temperature. Consequently, stretching modes related to cobalt and CN were proven to be highly anharmonic out of all other traced modes in the trigonal phase of $Ag_3Co(CN)_6$[26,28].

SnSe crystallizes in orthorhombic layered structure (*Pnma* space group) at low temperatures.Each layer contains zigzag planes of Sn-Se which is extended into two directions. The network generated from covalent bonds forms the double layer in the material. The Sn atoms orient at the off-center of the rectangle formed by Se atoms. With increasing temperature, Sn atoms drift towards the center of the Se rectangle and eventually at high temperature the crystal undergoes phase transition into *Cmcm* phase[29].

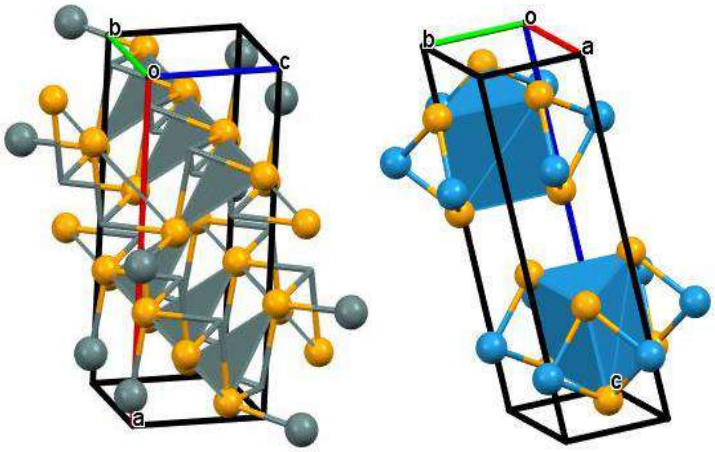

(a) (b)

Figure 14: The crystal structure of (a) SnSe[29]and (b) 2H-WS_2[30]

The presence of strong anharmonicity also results in ultralow thermal conductivity observed in single crystalline SnSe. Temperature dependent Raman studies (77K to 800K) exhibited softening of optical phonons (between ~70and150cm^{-1}) six times more along b-c plane in comparison to an axis. The magnitudes of cubic and quartic anharmonicity were calculated and FWHM and peak frequencies of these phonon modes were plotted as a function of temperature which proved that the cubic term of the true anharmonicity is responsible for the phonon decay in this material[23]. Another similar approach was adapted in the study of phonon behavior of Tungsten Disulfide consisting of multiple layer of S-W-S. Each S-W-S layer contains W atom enclosed in a 2D hexagonal lattices formed by six S atoms around it[24,30]. Temperature Dependent Raman Study was performed on Tungsten

Disulfide (2H-WS_2) over a temperature range of 3.6K to 850K. Frequency dependence and FWHM as a function of temperature shows nonlinear red shifts of all the phonons and broadening of linewidths respectively which is a consequence of phonon-phonon interaction (true anharmonicity). Softening of low optical phonons was traced over whole temperature range. At lower temperatures, Softening was found to be dominated by three phonon process while at high temperatures; four phonon processes played the active role in phonon decay in 2H-WS_2. This was in agreement of the results of Density of phonon states[24].

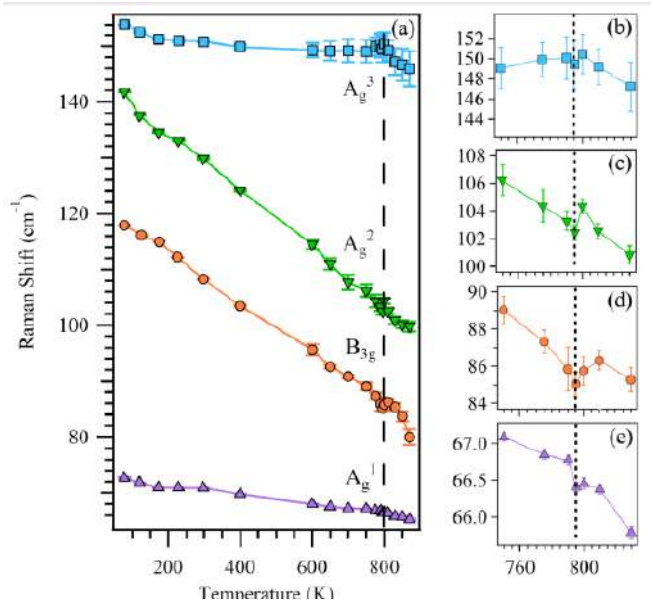

(a)

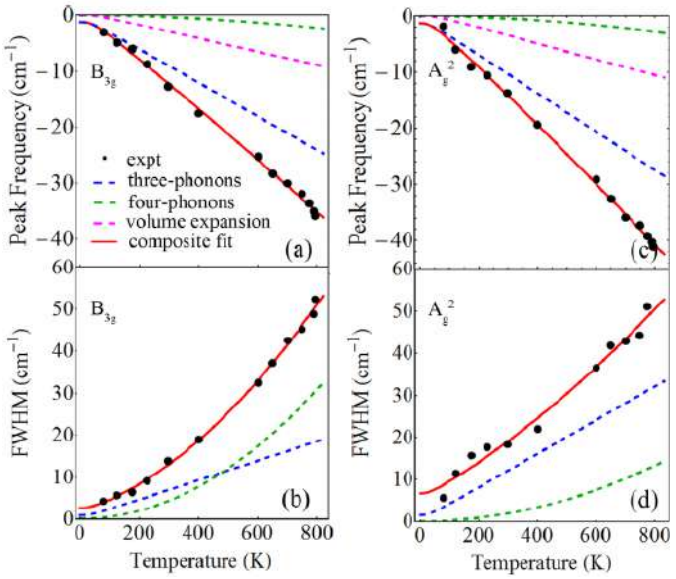

(b)

Figure 15:Thermal response ofA_g^1, B_{3g}, A_g^2 and A_g^3phonon modes of SnSe (a)Raman spectra of the above mentioned phonon modes in the Left panel and their zoomed view in the right panel (b)Frequency variation and FWHM[23].

"Reused (figure 2 and 3) with permission from [Liu, F., Parajuli, P., Rao, R., Wei, P. C., Karunarathne, A., Bhattacharya, S., Podila, R., He, J., Maruyama, B., Priyadarshan, G., Gladden, J. R., Chen, Y. Y., & Rao, A. M. (2018). Phonon anharmonicity in single-crystalline SnSe. *Physical Review B*, *98*(22).] Copyright (20018) by the American Physical Society."

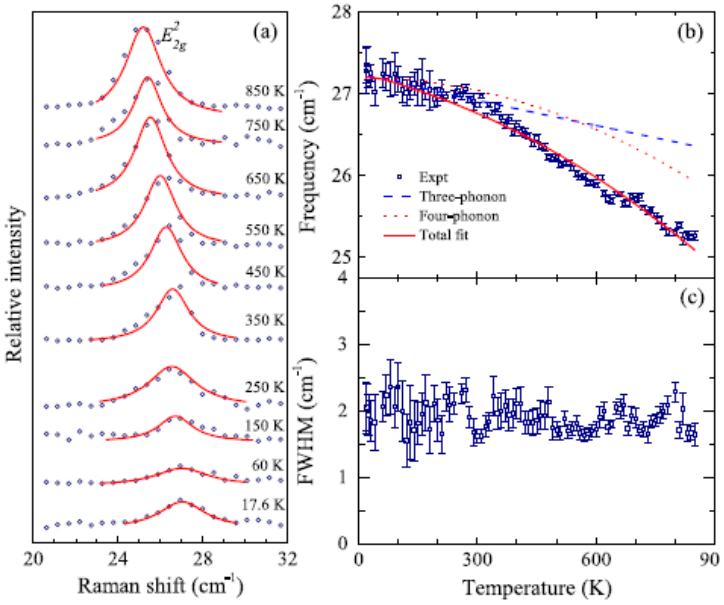

(a)

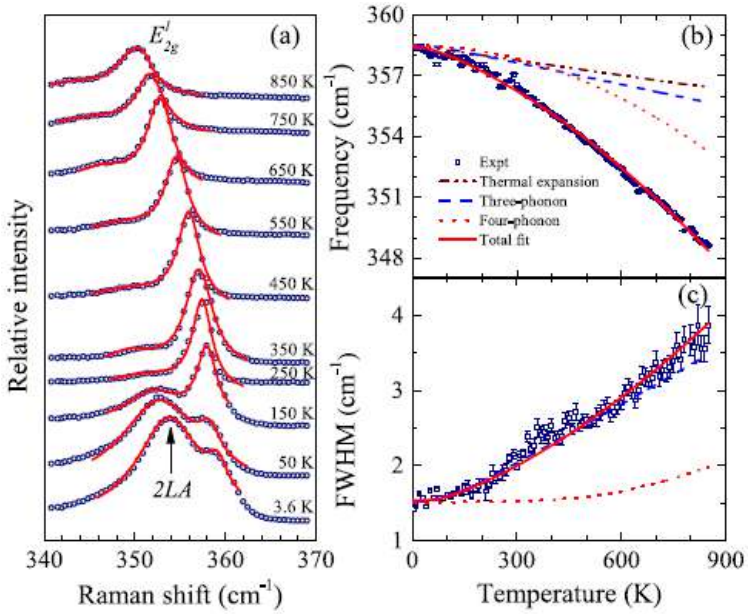

(b)

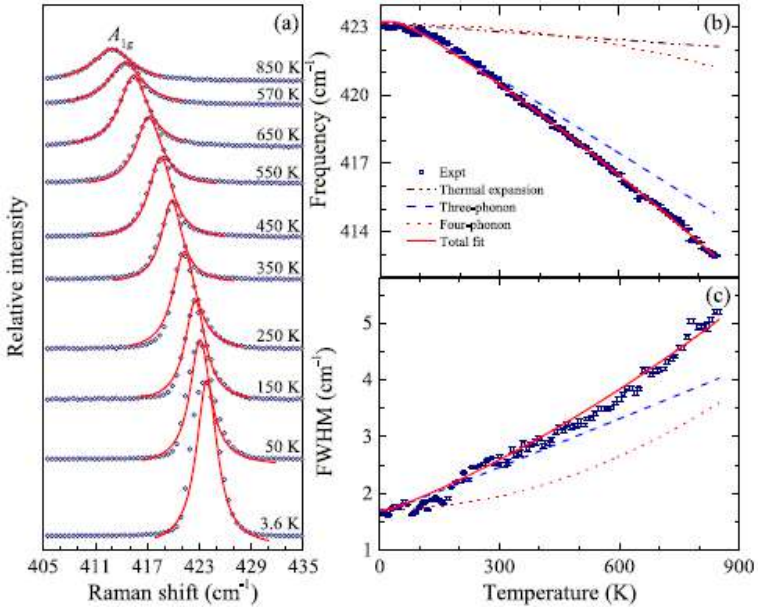

(c)

Figure 16: Thermal response ofE^2_{2g}, E^1_{2g} and A^1_g phonon modes of 2H-WS_2 (a)Raman spectra (b)Frequency variation and (c)FWHM[24].

"Reused (adapted) with permission from {Peng, Y. K., Cao, Z. Y., Chen, L. C., Dai, N., Sun, Y., & Chen, X. J. (2019). Phonon Anharmonicity of Tungsten Disulfide.

Journal of Physical Chemistry C, 123(41), 25509–25514.}Copyright {2019}American Physical Society."

2. Analytical Method:

As discussed in the second method, phonon mode frequencies can be interpreted as a function of temperature and pressure. A graphical approach called Zallen and Conwell method is an alternative way to analyze the anharmonicity of phonon modes. The plot of $\partial\omega_j/_{\partial \mathrm{P}}$ vs $d\omega_j/_{\mathrm{dT}}$ for several modes gives out the visualization of anharmonicity. Thus, one can obtain the phonon modes which are strongly anharmonic for a material by plotting their quasi-anharmonic and total temperature dependent components. As described by Zallen and Conwell, an implicit factor (η, dimensionless parameter) can be defined as follows

$$\eta = -\frac{\partial\omega}{\partial P}\left(\frac{d\omega}{dT}\right)^{-1}\left(\frac{\alpha}{\beta}\right) \qquad (23)$$

Where $\beta = -V^{-1}\left(\partial V/_{\partial P}\right)$ defines the isothermic compressibility. For the case where quasi-anharmonic dominates, the temperature and pressure effects resemble each other and $\frac{\partial\omega}{\partial P}\left(\frac{d\omega}{dT}\right)^{-1}$ equals to the$\left(\frac{\beta}{\alpha}\right)$. Hence, in such a case η =1. On the other hand, η =0 describes that the modes have purely true anharmonic contribution. If both (true and quasi contributions) are comparable and possesses same sign then the implicit fraction has a magnitude of 0.5. In a similar manner, one can draw various constant lines of η to realize the specific contributions of anharmonicity[10, 32].

Figure shows the Zallen and Conwell plot for Zirconium Tungstate. The constant lines of various η for the traced modes of zirconium tungstate were examined. For PTE materials modes lies in the fourth quadrant which was found to be shifted in the second quadrant in this material. For most of the modes (41 cm^{-1},144 cm^{-1},308 cm^{-1},381 cm^{-1},333 cm^{-1}) the upwards shift is observed with temperature and for the modes (84 cm^{-1} and 64cm^{-1}) downward shift is observed with pressure indicating NTE behavior in this material. The latter modes were stated to be dominated by true anharmonicity whereas the former one has quasi-anharmonic contribution. The 64cm^{-1} mode and 84cm^{-1}modes (typically) have been marked for exhibiting largest total anharmonicity in this material[10].

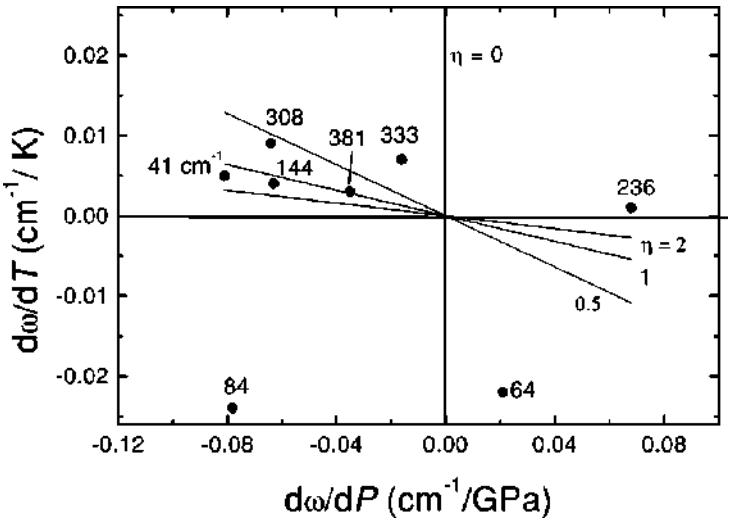

Figure 17: Zallen and Conwell plot ZrW_2O_8 describing Anharmonic contributions of the phonon modes of ZrW_2O_8[10].

"Reused (figure 3) with permission from [Ravindran, T. R., Arora, A. K., & Mary, T. A. (2003). Anharmonicity and negative thermalexpansion in zirconium tungstate. *Physical Review B - Condensed Matter and Materials Physics*, *67*(6), 1–4.] Copyright (2003) by the American Physical Society."

Theoretical Method:

Density Functional theory based ab-initio calculations help to encounter quantities such as band structure, force, pressure etc. Phonons have energy scale ranging from 1-500meV. From Density Functional (DFT) calculations, phonon frequencies and also the phonon dispersion inside the Brillouin zone characteristic of a crystalline solid can be obtained. One can further investigate quasi-anharmonic contribution offered by the lattice dynamics in a material[11,32]. Now, we present some insights into contribution of phonon modes of the two materials (β-eucryptite and ReO_3) with RUMs as a root cause for NTE interpreted by DFT calculations. A variety of materials with source of NTE other than RUMs such as $Ag_3Co(CN)_6$, ScF_3, CuX (X= halides) etc have been extensively studied using DFT calculations.

β-eucryptite ($LiAlSiO_4$) consists of double helices of SiO_4 and AlO_4tetrahedraproviding alternating layers of Al and Si perpendicular to c-axis. Primary channel consists of Li1 atoms while Li2 and Li3 atoms comprise of secondary channel type oriented along different

axes in the unit cell. Li sitting in 1D parallel to c-axis. Single unit cell has six tetrahedra available i.e. three secondary and one primary channel. But only three available sites are occupied in an alternating fashion at room temperature. This material shows strong anisotropic NTE between the temperature range of 300-1400K[11, 33].

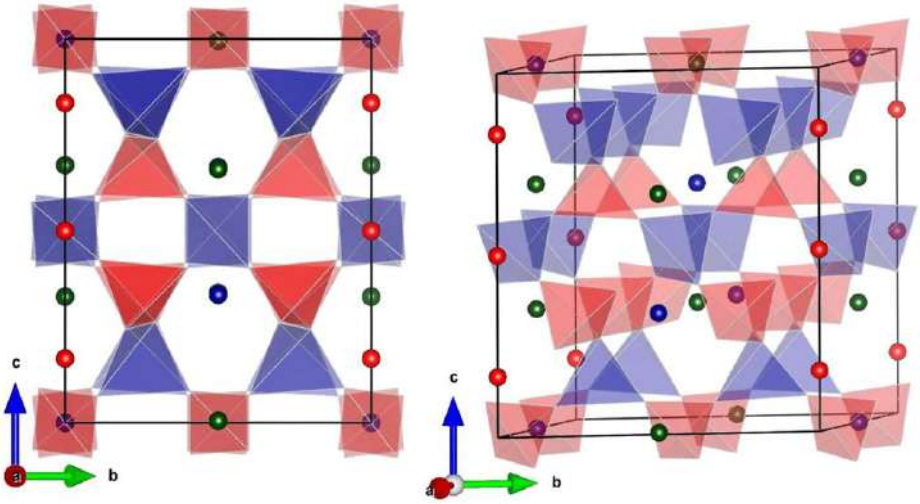

Figure 18: The crystal structure of β-eucryptite[34].

"Reused from [Singh, B., Gupta, M. K., Mittal, R., Zbiri, M., Rols, S., Patwe, S. J., Achary, S. N., Schober, H., Tyagi, A. K., & Chaplot, S. L. (2017). Role of phonons in negative thermal expansion and high pressure phase transitions in β-eucryptite: An ab-initio lattice dynamics and inelastic neutron scattering study. *Journal of Applied Physics*, *121*(8).], with the permission of AIP publishing."

Single crystal X-ray diffraction (SCXRD) and Raman studies have shown pressure induced transition for this material at 0.8 GPa and 300 K. High pressure XRD studies have stated that it involves phase transition from hexagonal to orthorhombic phase between 0.83 GPa and 1.12 GPa, while with higher pressure ~4.5 GPa it becomes amorphous. Experimental inelastic neutron scattering spectra was analyzed with the help of ab-initio DFT in order to understand lattice dynamics, as shown in figure19. It can be noticed that phonon modes can be distinguished in two distinct regimes extended up to 100meV and 110-150meV respectively. The first regime involves vibrations of all the atoms of the unit cell while another high-energy spectrum part involves internal vibrations of the SiO_4 and AlO_4 tetrahedra. The understanding of vibrations of individual atoms in the neutron inelastic spectrum (Figure19) was given by calculating Partial Density of States (PDOS). The calculated mean square amplitude for all the

atoms was then analyzed with the variation of energy and temperature, and it was found that since Li and O are lighter atoms with larger amplitude they can serve in polyhedral motion of this material[11,34].

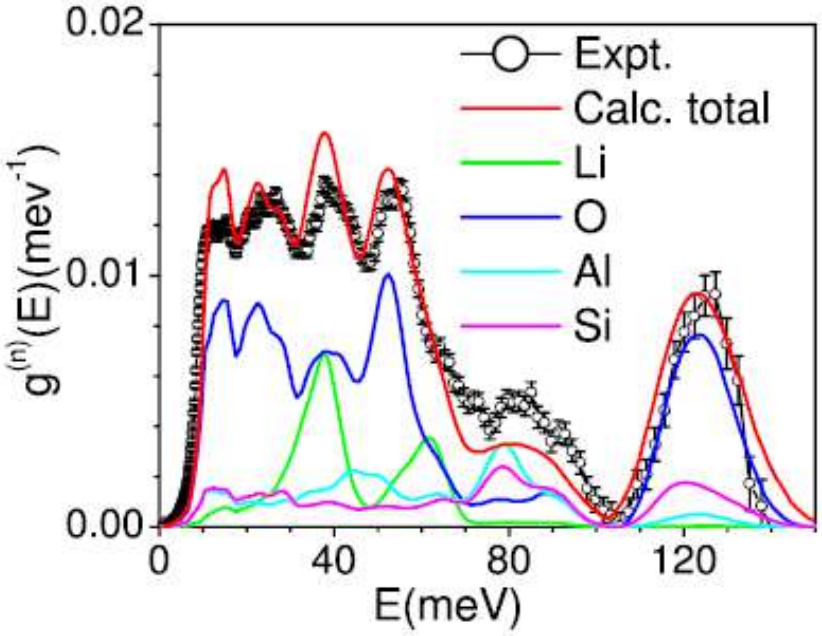

Figure 19: Plot of partial density of states verses energy in β-eucryptite describing individual atomic contribution by comparing experimental (inelastic neutron scattering and calculated (ab- inito) data[34].

"Reproduced from [Singh, B., Gupta, M. K., Mittal, R., Zbiri, M., Rols, S., Patwe, S. J., Achary, S. N., Schober, H., Tyagi, A. K., & Chaplot, S. L. (2017). Role of phonons in negative thermal expansion and high pressure phase transitions in β-eucryptite: An ab-initio lattice dynamics and inelastic neutron scattering study. *Journal of Applied Physics*, *121*(8).], with the permission of AIP publishing."

Anomalous Thermal Expansion in this material required knowledge of Grüneisen parameter $\gamma_l(E_{q,i}) = -\left(\frac{\partial ln E_{q,i}}{\partial ln l}\right)_{T,l'}; l, l' = a, b, c \;\&\; l' \neq l$ obtained for entire Brillouin zone. For hexagonal system, $\gamma_a = \gamma_b$ .Hence, γ_a and γ_c variation as a function $E_{q,i}$ (describing q-point energy of i^{th} phonon mode in Brillouin zone) showed large negative Γ magnitudes for low energy phonons(~10meV) while positive magnitudes for high energy phonons (30-70meV). The observed anisotropy in γ and calculated elastic constants suggested anisotropic NTE in the material. Hence, volume thermal expansion coefficient ($\alpha_v = (2\alpha_a + \alpha_c)$) was then

calculated using calculated values of linear thermal coefficient$\alpha_a$andα_c *as mentioned in Ref*34). $\alpha_v$along a-b plane was found to be negative for low temperatures and positive for high temperature. The deviation of calculated lattice parameters from the experimental data at 600K indicated the presence of anharmonicity. Consequently, this material behaved as NTE(α_v = - 1.7×10^{-6} K^{-1}) below 300K and PTE at high temperatures. To find out the specific mode causing NTE in this material, phonon dispersion at ambient as well as 0.5GPa was constructed. Among all the modes of the Brillouin, $\gamma_a$and $\gamma_c$turned out as negative resulting into NTE along a and c at low temperatures. On the other hand, at high temperatures it showed PTE in a-b plane and NTE in c-axis. The polarization vectors for soft modes were visualized further in order to understand their internal vibrations along the three Cartesian axes. Large negative values for γ_a and γ_c belonged to two modes. 1. M-point involving sliding motion of SiO_4 in a-b plane, AlO_4 polyhedral rotation and movement of Li atoms along b and c axes. 2. A-point: AlO_4ploryhedral rotation about a-axis, SiO_4ploryhedral rotation about b-axis and Li movement in a-b plane. The calculated eigen values for these M and A point phonon modes showed softening in the entire Brillouin zone obtained at 0GPa and 2GPa. This can be the driving point for phase transition in the material. Hence, it is concluded that AlO_4 and SiO_4 polyhedral rotation along a and c axes are responsible for NTE at low temperatures in this material[34]

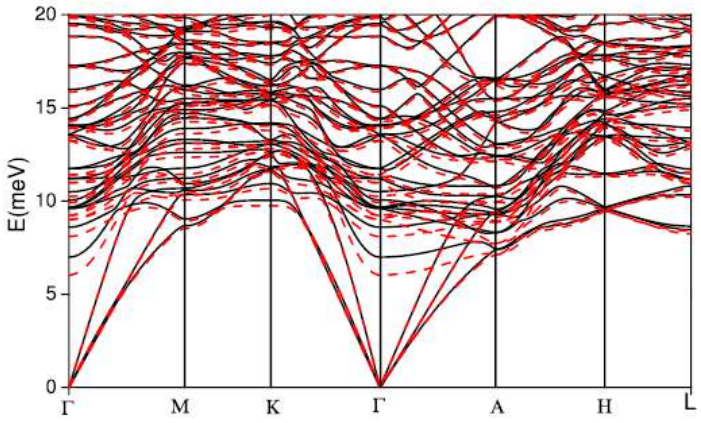

Figure 20: The contribution to phonon dispersion spectra offered by High symmetry directions in Brillouin zone of the unit cell of β-eucryptite at ambient (solid lines) and 0.5GPa (dashed lines) [34].

ReO_3 is a simple perovskite like cubic structure of ReO_3 (transition metallic oxide) consists of corner-linked ReO_6 octahedral units having Re at the centers and Re-O-Re linear linkages[11,35].

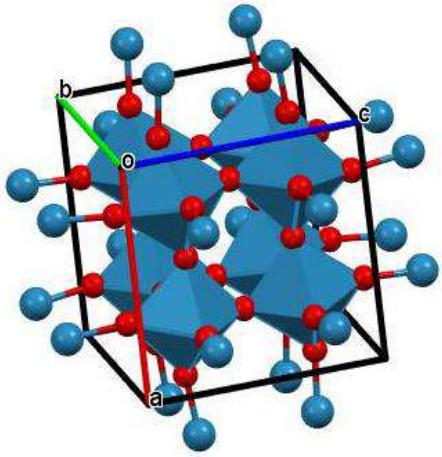

Figure 21: The crystal structure of ReO_3[35]

The structure of $ReO_3$is comprised of linear linkages of Re-O-Re and corner linked ReO_6 octahedra having Re centered in the octahedra[35].It shows phase transition from cubic(I) phase $Pm3m$-monoclinic phase $C2/C$-rhombohedral I phase- rhombohedral II phase as marked through Raman and X-ray diffraction studies over high pressures but there was a large disparity observed between obtained and theoretical phonon frequencies. This variance of the phonon mode frequencies is observed due to electron phonon coupling and anharmonicity. The dissimilarity was tackled using DFT over high symmetry points (Γ, X, M and R) in the Brillouin zone of ReO_3.The phonons along M, R and X points were traced to reveal softening. The M-point belongs to the rotation of ReO_6 octahedron along z-axis and is triply degenerating similar to R_{25} mode involving rotation of ReO_6 octahedron along each of the axes. Instability in either of the above two modes (M_3 and R_{25}) have a tendency for the phase transition occurrence in the material. Among all of the soft optical modes, M_3 and R_{25} only showed strong anomaly as a function of pressure giving out signatures of structural transitions. The transition pressure

between $Pm3m$ and $Im3$ phase was obtained as 0.5 ± 0.1 GPa based upon calculated enthalpies of the modes at different pressures. This was the pressure where M_3 loses its stability. Further it was realized that the transverse (TA) and longitudinal (LA) acoustic modes' coupling to M_3 modes take part in the phase transition.M_3 phonons achieve instability at P>3GPa and phase transition was noticed at lower pressure of 0.5GPa. Previous reports[37, 38]shows that ω^2 is related to phase transition pressure by the relation: $\omega^2 \alpha (P-P_c)$ where P_c is a phase transition pressure and $P< P_c$, following the mean field theory. At the transition pressure, ω^2 corresponding to the soft phonons approaches to a very low value signifying the first order phase transition. Thus, the ω^2 vs P plot for M_3 mode was thereafter analyzed in order to understand the behavior of M_3 soft phonon mode across phase transition. It was observed that there is a discontinuity of slope value for ω^2 for M_3 phonon mode at 0.5GPa and anon-zero magnitude of phonon frequency at 0.5GPa. Moreover, the observed M_3 phonon mode frequency for pressure just lower to transition pressure was found to be $64cm^{-1}$. Such a low phonon frequency signified that the transition is of weakly first order.[36].

Neutron diffraction studies of Chatterji et.al.[39]on thermal behavior of ReO_3 found that unusual NTE property is a result of increased anharmonicity in the M_3 mode. It has been witnessed that there is a continuous decrement of lattice parameter with increasing temperature up to 200K. After crossing this temperature, the material again shows normal thermal expansion (PTE) upto the measured temperature of 305K. Further, the atomic displacement parameters of Re and O atoms with change in temperature revealed that vibrations in O atoms are thermally strong. Lattice dynamical analysis suggested that major contribution for NTE in this material comprises of low energy phonons (~14meV), typically belonging to M_3 mode in the Brillouin zone[39].

Significant gaps in the research

Present article focuses on the types of methodologies helpful for understanding the lattice dynamics of NTE materials. Several other techniques such as Inelastic X-ray scattering and Infra-red scattering can also be explored to study the aspect of Anharmonicity in an NTE material. Various families of NTE materials namely metal cyanides, coordinated cyanometalletes polymers, nanostructures, family of halides can also be explored for the detailed investigation in this direction.

Conclusion and Future Directions

In Summary, phonon anharmonicity plays a vital role in understanding the thermal properties of a system. Three methods namely, experimental, analytical and theoretical are discussed in this article to understand the phonon anharmonicity. As discussed, Specific heat dependency with Grüneisen parameter and ab-initio calculations of DFT can be approached to understand the phonon behavior as a function of pressure. Brillouin zone of the phonon spectrum can also be beneficial to the researchers for exploring the phonon anharmonicity. Further contribution of anharmonicity can be studied with Zallen-Conwell plot. Presently discussed examples show that low energy phonons with large negative γ_i cause NTE in the material involving transverse vibrations, liberations and internal distortions of rigid unit modes. In majority of the materials presented in this article, true anharmonicity is the key factor which dominates for strong anharmonicity, typically the quartic or four phonon contribution. Another family of metal cyanides has attracted scientists to inspect their thermal properties. Several compounds such as $HgCN(NO_3)$, CuCN, AgCNetc[40,41,42]have been reported as NTE materials. Investigations of phonon anharmonicity in these compounds can help understand the cause for their NTE behavior. Apart from metal cyanides, family of fluorides and nanostructures NTE materials can be explored in detail[40, 41, 42, 43, 44].

References

1. Dekker, A. J. (1958). Solid State Physics, Vol. 6. *Progress in Materials Science, 92*, 360–445
2. Rangarajan, G., & Vijaya, M. S. (2004). *Materials science*. Tata McGraw-Hill Education.
3. Stidham, H. D. (2017). Heat Capacities of Solids. *Statistical Thermodynamics for Beginners*,431–479. https://doi.org/10.1142/9789813149946_0016
4. Garai, J. (2007). Physics behind the Debye temperature.*arXiv: Chemical Physics, 3*(1), 1-8. Retrieve fromhttps://arxiv.org/abs/physics/0703001
5. *Debye specific heat*. (n.d.). https://commons.wikimedia.org/wiki/File:DebyeVSEinstein-ruRu.png

6. *Ulmpkapp process*.(n.d). *https://commons.wikimedia.org/wiki/File:Phonon_nu_process.png*
7. *Monoatomic dispersion*. (n.d.). https://search.creativecommons.org/photos/7cfa6c60-b1a4- 415c-bf5f-8bfaf43de579
8. *Dispersion curve of a Diatomic lattice*. (n.d.). https://search.creativecommons.org/photos/e241e9a9-aa09-490f-a4ab-cdbe6829cf3e
9. Eyring, E. M. (1978). Topics in Applied Physics. *In Nuclear Technology*, *39*(3), 327-328. https://www.tandfonline.com/doi/abs/10.13182/NT78-A32063
10. Ravindran, T. R., Arora, A. K., & Mary, T. A. (2003). Anharmonicity and negative thermalexpansion in zirconium tungstate. *Physical Review B*, *67*(6), 1–4. https://doi.org/10.1103/PhysRevB.67.064301
11. Mittal, R., Gupta, M. K., & Chaplot, S. L. (2018). Phonons and anomalous thermal expansion behaviour in crystalline solids. *Progress in Materials Science*, *92*, 360–445
12. Piovano, A. (2015). Inelastic neutron scattering applied to materials for energy. *EPJ Web of Conferences*, *104*, 01006-p.1-01006-p.17.https://doi.org/10.1051/epjconf/201510401006(This is an Open Access article distributed under the terms of the Creative Commons Attribution License 4.0)
13. Evans, J. S. O., Mary, T. A., Vogt, T., Subramanian, M. A., & Sleight, A. W. (1996). Negative Thermal Expansion in ZrW 2 O 8 and HfW 2 O 8. *Chemistry of Materials*, *8*(12), 2809–2823. http://pubs.acs.org/doi/pdf/10.1021/cm9602959.
14. Ernst, G., Broholm, C., Kowach, G. R., & Ramirez, A. P. (1998). Phonon density of states and negative thermal expansion in ZrW 2 O 8. *Nature*, *396*(6707), 147–149.
15. Ramirez, A. P., & Kowach, G. R. (1998). Large Low Temperature Specific Heat in the Negative Thermal Expansion Compound ZrW_2O_8. *Physical Review Letters, 80*(22), 4903–4906.https://doi.org/10.1103/PhysRevLett.80.4903
16. Ravindran, T. R., Arora, A. K., & Mary, T. A. (2000). High pressure behavior of ZrW2O8: Grüneisen parameter and thermal properties. *Physical Review Letters*, *84*(17), 3879–3882. https://doi.org/10.1103/PhysRevLett.84.3879
17. Ravindran, T. R., Arora, A. K., & Mary, T. A. (2001). High-pressure Raman spectroscopic study of zirconium tungstate. *Journal of Physics Condensed Matter*, *13*(50), 11573–11588. https://doi.org/10.1088/0953-8984/13/50/316
18. Tucker, M. G., Goodwin, A. L., Dove, M. T., Keen, D. A., Wells, S. A., & Evans, J. S.

O. (2005). Negative thermal expansion in ZrW 2O 8: Mechanisms, rigid unit modes, and neutron total scattering. *Physical Review Letters*, *95*(25), 8–11. https://doi.org/10.1103/PhysRevLett.95.255501

19. Ravindran, T. R., Arora, A. K., Chandra, S., Valsakumar, M. C., & Shekar, N. V. C. (2007). Soft modes and negative thermal expansion in Zn (C N) 2 from Raman spectroscopy and first-principles calculations. *Physical Review B*, *76*(5), 54302.
20. Goodwin, A. L., & Kepert, C. J. (2005). Negative thermal expansion and low-frequency modes in cyanide-bridged framework materials. *Physical Review B*, *71*(14), 1–4. https://doi.org/10.1103/PhysRevB.71.140301
21. Chapman, K. W., & Chupas, P. J. (2007). Pressure enhancement of negative thermal expansion behavior and induced framework softening in zinc cyanide. *Journal of the American Chemical Society*, *129*(33), 10090–10091. https://doi.org/10.1021/ja073791e
22. Mittal, R., Chaplot, S. L., & Schober, H. (2009). Measurement of anharmonicity of phonons in the negative thermal expansion compound Zn (CN) 2 by high pressure inelastic neutron scattering. *Applied Physics Letters*, *95*(20), 2007–2010. https://doi.org/10.1063/1.3264963
23. Liu, F., Parajuli, P., Rao, R., Wei, P. C., Karunarathne, A., Bhattacharya, S., Podila, R., He, J., Maruyama, B., Priyadarshan, G., Gladden, J. R., Chen, Y. Y., & Rao, A. M. (2018). Phonon anharmonicity in single-crystalline SnSe. *Physical Review B*, *98*(22), 2240309-1-2240309-7.https://doi.org/10.1103/PhysRevB.98.224309
24. Peng, Y. K., Cao, Z. Y., Chen, L. C., Dai, N., Sun, Y., & Chen, X. J. (2019). Phonon Anharmonicity of Tungsten Disulfide. *Journal of Physical Chemistry C*, *123*(41), 25509–25514. https://doi.org/10.1021/acs.jpcc.9b07553
25. Sood, A. K., Arora, A. K., Umadevi, V., & Venkataraman, G. (1981). Raman study of temperature dependence of lattice modes in calcite. *Pramana*, *16*(1), 1-16. https://link.springer.com/article/10.1007/BF02847889
26. Goodwin, A. L., Calleja, M., Conterio, M. J., Dove, M. T., Evans, J. S. O., Keen, D. A., Peters, L., & Tucker, M. G. (2008). Colossal positive and negative thermal expansion in the framework material Ag3[Co(CN)6]. *Science*, *319*(5864), 794–797. https://doi.org/10.1126/science.1151442
27. Pauling, L., & Pauling, P. (1968). A trireticulate crystal structure: trihydrogen cobalticyanide and trisilver cobalticyanide. *Proceedings of the National Academy of*

Sciences of the United States of America, *60*(2), 362.

28. Rao, R., Achary, S. N., Tyagi, A. K., & Sakuntala, T. (2011). Raman spectroscopic study of high-pressure behavior of Ag 3[Co(CN)6]. *Physical Review B*, *84*(5), 2–7. https://doi.org/10.1103/PhysRevB.84.054107
29. Sist, M., Zhang, J., & Iversen, B. B. (2016). Crystal structure and phase transition of thermoelectric SnSe. *Acta Crystallographica Section B: Structural Science, Crystal Engineering and Materials*, *72(3)*,310-316.
30. Schutte, W. J., De Boer, J. L., & Jellinek, F. (1987). Crystal structures of tungsten disulfide and diselenide. *Journal of Solid State Chemistry*, *70*(2), 207-209. https://doi.org/10.1016/0022-4596(87)90057-0
31. Zallen, R., & Conwell, E. M. (1979). The Effect of temperature on Libron Frequencies in molecular crystals: Implications for TTF-TCNQ. *Solid State Communications*, *31*(8), 557-561. https://doi.org/10.1016/0038-1098(79)90252-7
32. Hasnip, P. J., Refson, K., Probert, M. I. J., Yates, J. R., Clark, S. J., & Pickard, C. J. (2014). Density functional theory in the solid state. *Philosophical Transactions of the Royal Society A: Mathematical, Physical and Engineering Sciences*, *372*(2011). https://doi.org/10.1098/rsta.2013.0270
33. Pillars, W. W., & Peacor, D. R. (1973). The Crystal Structure of Beta Eucryptite as a Function of Temperature. *American Mineralogist*, *58*(1972), 681–690. http://www.minsocam.org/ammin/AM58/AM58_681.pdf
34. Singh, B., Gupta, M. K., Mittal, R., Zbiri, M., Rols, S., Patwe, S. J., Achary, S. N., Schober, H., Tyagi, A. K., & Chaplot, S. L. (2017). Role of phonons in negative thermal expansion and high pressure phase transitions in β-eucryptite: An ab-initio lattice dynamics and inelastic neutron scattering study. *Journal of Applied Physics*, *121*(8). https://doi.org/10.1063/1.4977244
35. Schirber, J. E., Morosin, B., Alkire, R. W., Larson, A. C., & Vergamini, P. J. (1984). Structure of ReO3 above the "compressibility collapse" transition. *Physical Review B*, *29*(7), 4150–4152. https://doi.org/10.1103/PhysRevB.29.4150
36. Muthu, D. V. S., Teredesai, P., Saha, S., Suchitra, Waghmare, U. V., Sood, A. K., & Rao, C. N. R. (2015). Pressure-induced structural phase transitions and phonon anomalies in Re O3: Raman and first-principles study. *Physical Review B*, *91*(22), 1–8. https://doi.org/10.1103/PhysRevB.91.224308

37. Mishra, K. K., Ravindran, T. R., Island, J. O., Flores, E., Ares, J. R., Sanchez, C., Ferrer, I. J., van der Zant, H. S. J., Pawbake, A., Kanawade, R., Castellanos-Gomez, A., & Late, D. J. (2020). Raman Fingerprint of Pressure-Induced Phase Transitions in TiS3 Nanoribbons: Implications for Thermal Measurements under Extreme Stress Conditions. *ACS Applied Nano Materials*, *3*(9), 8794–8802. https://doi.org/10.1021/acsanm.0c01583
38. Cochran, W. (1959). Crystal Stability and the Theory of Ferroelectricity. *Physical Review Letters*, *3*(9), 412–414. https://doi.org/10.1103/physrevlett.3.412
39. Chatterji, T., Henry, P. F., Mittal, R., & Chaplot, S. L. (2008). Negative thermal expansion ofReO3: Neutron diffraction experiments and dynamical lattice calculations. *Physical Review B*, *78*(13), 1341051- 1341056. https://doi.org/10.1103/physrevb.78.134105
40. Korčok, J. L., & Leznoff, D. B. (2013). Thermal expansion of mercury(II) cyanide and HgCN(NO3). *Polyhedron*, *52*, 72–77. https://doi.org/10.1016/j.poly.2012.11.038
41. Bowmaker, G. A., Kennedy, B. J., & Jason, C. R. (1988). Crystal Structures of AuCN andAgCN and Vibrational Spectroscopic Studies of AuCN, AgCN, and CuCN. *Inorganic Chemistry*, *37*(16), 3968-3974. https://doi.org/10.1021/ic9714697
42. Jain, A., Ghalsasi, P. S., & Ghalsasi, P. (2021). Back-bonding driven negative thermal expansion along the one dimensional Hg C N linkage in [HgCN](NO3) probed by Raman spectroscopy. *Polyhedron*, *205*(12), 115293. https://doi.org/10.1016/j.poly.2021.115293
43. Wang, L., Cong, W., Sun, Y., Kewen, S., Sihao, D., Huiqing, L., Pengwei, H., & Xiaoyun, Z. (2015). Metal fluorides, a new family of negative thermal expansion materials. *Journal of Materiomics*, *1*(2), 106-112.https://doi.org/10.1016/j.jmat.2015.02.001
44. Jiang, J. W., Wang, J. S. & Baowen, Li. (2009). Thermal expansion in single-walled carbon nanotubes and graphene: Nonequilibrium Green's function approach. *Physical Review B, 80*(20), 1-7. https://doi.org/10.1103/PhysRevB.80.205429

Glossary:

Bulk Modulus- The property of resisting to compression in a material

Specific molar heat- The total portion of heat energy contributing to increase the temperature by 1K for 1mole of a material

Inelastic neutron scattering- It is an experimental technique to understand atomic and molecular behavior of a material. It determines the variation in kinetic energy achieved due to the inelastic collision between the neutrons and the sample.

Phonon density of states- Total number of phonon energy levels per unit energy per unit volume

Thermal resistance- A property of a material to resist a flow of heat. It is an inverse of thermal conductance.

Harmonic oscillator- It describes a system which dis-orients its equilibrium position when its restoring force is linearly varying to the displacement.

FWHM- The line shape width at the half of its maximum amplitude determines the full width at half maximum (FWHM).

Isothermic compressibility- It is the ratio of partial derivative of change in volume and partial derivative change in pressure at constant temperature.

Lattice- Imaginary grid to place atoms in a crystal

Crystal defects- It describes the state of lattice involving imperfections in the atomic arrangement deceased from regularity.